Liquid Viscosities of Methane and Propane

G. W. SWIFT, J. A. CHRISTY, and FRED KURATA

University of Kansas, Lawrence, Kansas

The theory and calibration procedure for a cylindrical falling body viscometer is presented.

Experimental viscosity data are given for liquid methane from −150°C. to the critical point and for liquid propane from −185° to +90°C. The maximum experimental error for methane data is ±8% and for propane data ±5%.

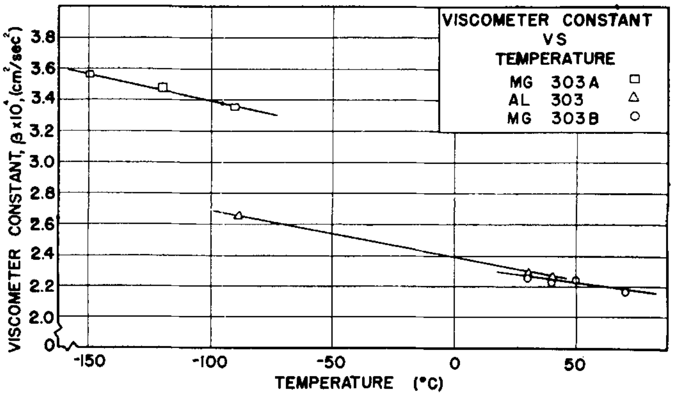

Fig. 1. Viscometer constant vs. temperature.

A literature survey shows that there are very few data on viscosities of normally gaseous hydrocarbons in the liquid phase above their normal boiling points. Data which are available have been obtained over limited ranges of temperature and pressure. Furthermore there has been no attempt made to consolidate the viscosity data for any hydrocarbon over the complete liquid region.

The data presented here range from from the normal boiling point to the critical point of the hydrocarbon tested. In addition, through calibration procedures, the data are consolidated with those of the American Petroleum Institute (*8*), which are given from the freezing point to the normal boiling point. The end result is a consistent set of viscosity data for methane and propane which extend over their entire liquid region.

The data which are presented here were obtained on the apparatus described by Swift, *et al.* (*11*).

THEORY AND EXPERIMENTAL APPLICATION

The theoretical basis for determining viscosity by the falling-body method comes from the work of Stokes (*10*), who solved the classical equations of hydrodynamics for the resistive force W, opposing the uniform motion of a sphere through an infinite, viscous medium. Stokes's equation is

$$W = 3\pi \, dv\mu \tag{1}$$

Rayleigh (*7*) pointed out that the assumptions leading to Equation (1) were valid only when the Reynolds number was less than unity. Barr (*1*) proposed that Equation (1) be modified by a shape factor, such that

$$W = 3\pi \, dv\mu / \delta \tag{2}$$

The shape factor, a measure of the effect of the geometry of the falling body on the resistive force, is defined for any falling body having three axes of symmetry.

If a cylindrical body with hemispherical ends is used for the falling body, it is possible to derive a formula relating the viscosity to other physical

Table 1. Description of Falling Bodies

Body number	MM285	MM300	MM308
Description	Hollow cylinder with hemispherical ends; one end of cylinder drilled to equalize pressure on inner and outer surfaces of cylinder.		
Materials of construction	Methyl methacrylate with stainless steel collar		
Nominal diameter, in.	0.285	0.300	0.308
Maximum taper, in.	±0.001	±0.001	±0.001
Length, in.	3 5/16	3 1/16	3 1/16
Density, g./cc.	0.234	0.309	0.237
Total volume, cc.	3.73	3.83	4.07
Void volume, cc.	3.13	2.96	3.34
Body number	MG303A	AL303	MG303B
Description	Solid Cylinder	Hollow cylinder with hemispherical ends	
Materials of construction	Magnesium	Aluminum 5052S alloy	Magnesium
Nominal diameter, in.	0.303	0.303	0.303
Maximum taper, in.	±0.003–0.005 in. on each cylinder.		
Length, in	2.00	1.70	1.70
Density, g./cc.	1.775	1.051	0.538

J. A. Christy is now with Esso Standard Oil Company, Baton Rouge, Louisiana.

Supplementary material has been deposited as document 5829 with the American Documentation Institute, Photoduplication Service, Library of Congress, Washington 25, D. C., and may be obtained for $1.25 for photoprints or $1.25 for 35-mm. microfilm.

properties which can be measured with comparative ease.

The volume of such a body is

$$V = \frac{\pi d^2}{2} (h/2 + d/3) \qquad (3)$$

When one assumes that the body is moving under the acceleration of gravity, the apparent force on the body in the downward direction is

$$\begin{aligned} &Vg(\sigma - \rho) \\ &= \frac{\pi d^2 g}{2} (h/2 + d/3)(\sigma - \rho) \end{aligned} \qquad (4)$$

If the body is falling at constant velocity, the apparent downward force may be equated to the resistive force:

$$\begin{aligned} W &= \frac{3\pi \, dv\mu}{\delta} \\ &= \frac{\pi d^2 g}{2} (h/2 + d/3)(\sigma - \rho) \end{aligned} \qquad (5)$$

When one solves for the viscosity,

$$\mu = \frac{dg\delta}{6v} (h/2 + d/3)(\sigma - \rho) \qquad (6)$$

Before Equation (6) is applied in experimental work, it is necessary to consider the assumptions made to complete its derivation:

1. An Infinite Medium

The use of a finite medium introduces two experimental errors, the *end* effect and the *wall* effect. Barr (*1*) treated the subject of the end effect and found that it could be neglected in finite systems if the velocity of fall was measured at a point removed several body lengths from the end of the containing vessel. He also presented several theoretical derivations in which the correction for wall effect was treated as a function of the diameter of the containing vessel and the diameter of the falling body. If the wall-effect correction is defined as $\psi(D, d)$, the equation for the resistive force is then

$$W = \frac{3\pi \, dv\mu}{\delta \psi(D, d)} \qquad (7)$$

As the ratio of d/D approaches unity, the average velocity of the fluid passing the falling body v is no longer equal to the velocity of the falling body s/θ. These velocities are related, however, by the continuity equation

$$\frac{v}{s/\theta} = \frac{d^2}{D^2 - d^2} \qquad (8)$$

The viscosity in a falling-body viscometer, where $0.5 < d/D < 1$, is

$$\mu = \frac{g\delta\psi(D, d)(h/2 + d/3)(D^2 - d^2)(\sigma - \rho)\theta}{6sd} \qquad (9)$$

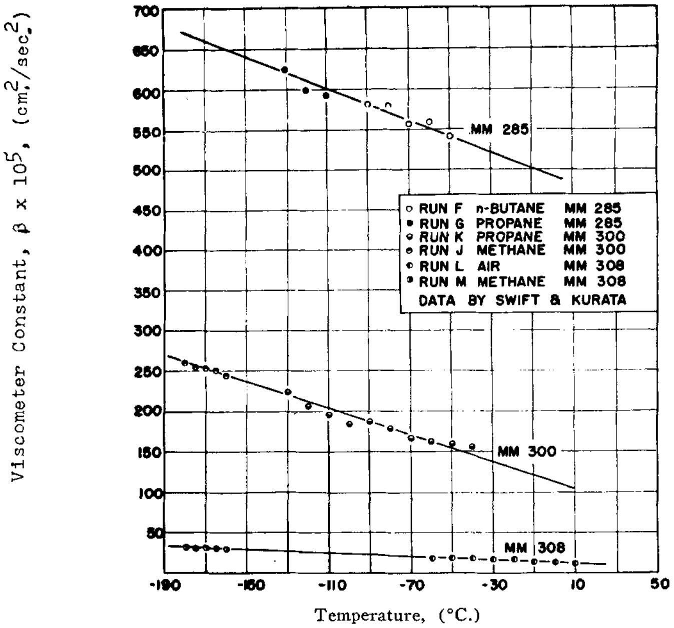

Fig. 2. Viscometer constant vs. temperature.

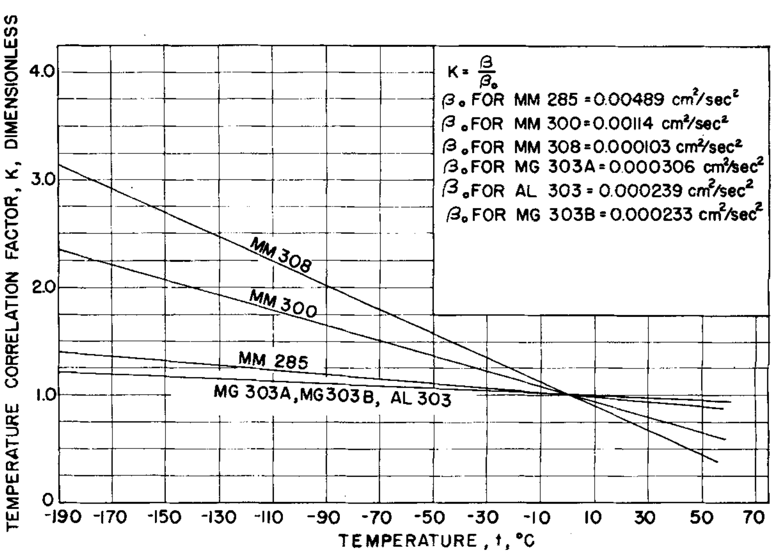

Fig. 3. Temperature correlation factor vs. temperature.

2. $\sigma > \rho$

The derivation implies that the density of the fluid is less than the density of the body. However the equations are equally valid for $\sigma < \rho$, the only difference being the reversal of the motion of the body.

3. Terminal Velocity of Fall

The velocity of the body approaches the limiting (terminal) velocity exponentially. By selecting the point for velocity measurement at a sufficient distance from the initial release point, one can eliminate error from this source.

4. $N_{Re} < 1$

To determine the Reynolds number at which laminar flow is terminated for falling spheres, Barr (*1*) described Castleman's method, that is, plotting the ratio of resistance per unit cross section to ρv^2 against N_{Re} on logarithmic coordinates. When data are plotted by this method, the points fall on a straight line as required by Stokes's Law for N_{Re} less than 1. Beyond this value of N_{Re} the resistance factor $f = 8W/\pi d^2 \rho v^2$ decreases less rapidly with increasing N_{Re} until it

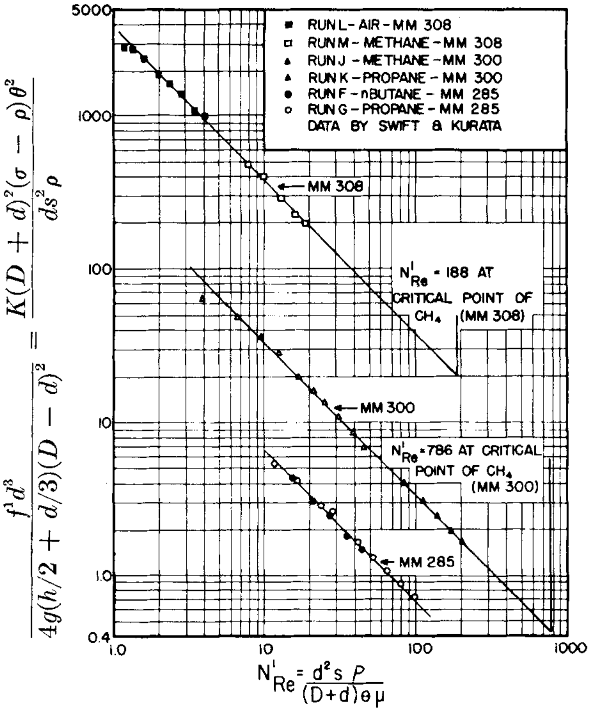

Fig. 4. Temperature corrected resistance function vs. modified Reynolds number.

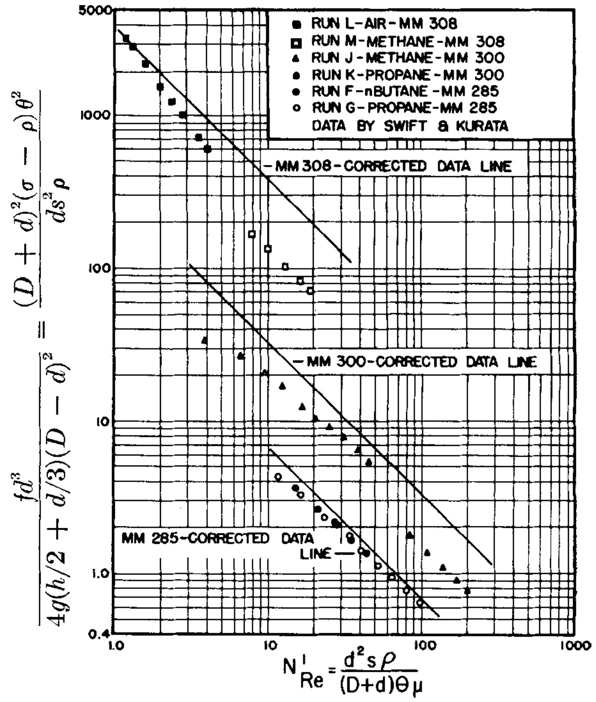

Fig. 5. Resistance function (not corrected for temperature) vs. modified Reynolds number.

becomes independent of viscosity and proportional to ρv^2. The break point at $N_{Re} = 1$ is the critical Reynolds number for viscometry, where $d/D \ll 1$.

Hubbard and Brown (*4*) plotted data similarly for a rolling-ball viscometry where the ratio of d/D approached unity, and then found that the critical modified Reynolds number was twenty. They used a modified Reynolds number

$$N_{Re'} = \frac{d^2 s\rho}{(D+d)\theta\mu} \tag{10}$$

to account for the equivalent diameter and the difference between fluid velocity and ball velocity.

Then, for a falling-cylinder viscometer, $0.5 < d/D < 1$

$$f = \frac{4g(D^2-d^2)^2(h/2+d/3)(\sigma-\rho)\theta^2}{\rho s^2 d^4} \tag{11}$$

A plot of the resistance factor [Equation (11)] vs. $N_{Re'}$ on logarithmic coordinates will determine the range of laminar flow for a cylindrical falling-body viscometer.

For precise experimental work Equation (9) is written

$$\mu = \beta(\sigma-\rho)\theta \tag{12}$$

where the viscometer calibration constant is determined experimentally. This practice is employed for accurate viscometric work because the physical dimensions of the apparatus cannot be measured with the desired accuracy; the wall-effect correction $\psi(D, d)$ is included in the calibration constant; the shape factor is included in the calibration constant; and the effect of temperature and pressure upon the dimensions of the apparatus can be determined and compensated for by considering $\beta = \phi(t, p)$.

Since

$$\beta = \frac{g\delta(D^2-d^2)(h/2+d/3)\psi(D,d)}{6sd} \tag{13}$$

Equation (11) may be rewritten

$$f = \frac{24\beta(D^2-d^2)(\sigma-\rho)\theta^2}{\delta\psi(D, d)\rho s d^3} \tag{14}$$

If β is a function of temperature, the data may be plotted with Equation (14) as the resistance factor. It is possible to use an alternate form by taking the value of β at some arbitrary temperature, say at 0°C., as was done here and computing the ratio $K = (\beta/\beta_0)$ for various temperatures. Then, substituting $\beta = K\beta_0$ into Equation (14) gives

$$f' = \frac{24\beta_0 K(D^2-d^2)(\sigma-\rho)\theta^2}{\delta\psi(D, d)\rho s d^3} = \frac{4gK(h/2+d/3)(D^2-d^2)^2(\sigma-\rho)\theta^2}{\rho s^2 d^4} \tag{15}$$

When the logarithm of the temperature-corrected resistance factor is plotted against the logarithm of the modified Reynolds number, the calibration data will be successfully correlated and the limits of laminar flow determined.

RESULTS

Experimental data were obtained by means of six falling bodies, the descriptions and dimensions of which appear in Table 1.

Densities of the cylinders MG303A, AL303, and MG303B were assumed to be constant at all temperatures and pressures. Any error in this assumption was compensated for in the experimental calibration constant. The densities of the methyl methacrylate cylinders varied with the densities of the fluids in which they were immersed. The apparent densities of these bodies were computed from a knowledge of the void volumes and total volumes of the bodies.

At least five, and usually ten, readings were obtained for every calibration and experimental fall time. The arithmetic means of these readings were used for computation.

Calibration of the viscometer for the various falling bodies was accomplished by determining experimental fall times in fluids of known viscosities. The accepted values of viscosity and density for the calibration substances, methane, propane, *n*-butane, and air, are given in the literature (*3, 5, 8*). The calibration procedure was carried out at various temperatures and pressures, so that the calibration constant might be expressed as a function of temperature and pressure. For any given temperature the effect of increasing pressure to 800 lb./sq.

TABLE 2. EXPERIMENTAL VISCOSITIES OF METHANE AND PROPANE

Substance	Temperature, °C.	Pressure, lb./sq. in. abs.	Body	$N_{Re'}$	Viscosity, centipoises	Phase
Methane	−150	350	MM308	20	0.0880	l
	−140	550		26	0.0734	
	−130	600		37	0.0599	
	−120	650		47	0.0508	
	−110	710		59	0.0435	
	−100	710		78	0.0357	
	− 95	710		86	0.0327	
	− 90	710		98	0.0294	
	− 85	710		122	0.0251	
	− 83.2	710		88	0.0249	Crit.
	− 83.2	710		100	0.0232	
	− 83.2	710		115	0.0214	
	− 80	695		118	0.0178	g
	− 76	685		209	0.0116	
	−150	365	MM300	234	0.0964	l
	−140	450		283	0.0768	
	−130	500		362	0.0660	
	−120	525		427	0.0578	
	−110	600		392	0.0589	
	−100	650		490	0.0496	
	− 95	700		583	0.0441	
	− 90	700		595	0.0421	
	− 85	700		681	0.0373	
	− 83.2	680		585	0.0346	Crit.
Propane	−185	50	MG303A	0.248	7.36	l
	−180	50		0.484	5.25	
	−170	50		1.58	2.96	
	−160	50		3.53	1.92	
	−150	50		7.13	1.34	
	−140	50		13.3	0.976	
	−130	50		21.5	0.761	
	−120	50		32.6	0.613	
	−110	50		46.4	0.510	
	−100	50		63.8	0.431	
	− 90	50	AL303	24.0	0.375	
	− 80	50		33.3	0.317	
	− 70	50		40.5	0.287	
	− 60	50		50.1	0.258	
	− 50	50		63.5	0.228	
	− 40	50		77.5	0.206	
	− 30	50		94.3	0.186	
	− 20	50		113	0.169	
	− 10	50		138	0.152	
	0	75		170	0.136	
	+ 10	95		196	0.126	
	+ 20	130		239	0.113	
	+ 30	170	MG303B	28.2	0.0987	
	+ 40	225		49.3	0.0845	
	+ 50	275		71.8	0.0766	
	+ 60	330		116	0.0646	
	+ 70	400		170	0.0575	
	+ 80	455		278	0.0478	
	+ 90	560		385	0.0427	

in. abs. had no effect on the fall time, an indication that moderate pressure did not affect either the measured viscosity or the physical dimensions of the viscometer, which is verified by Bridgeman (*2*). Plots of the viscometer calibration constant vs. temperature are presented in Figures 1 and 2.

A plot of K vs. t is presented in Figure 3. The values of K were computed from the most probable values of β for the various falling bodies.

A logarithmic plot of

$$\frac{[K(D + d)^2(\sigma - \rho)\theta^2]}{ds^2\rho}$$

vs. $N_{Re'}$ (Figure 4) is given using the calibration data. This plot shows that laminar flow existed in the viscometer during all calibration runs. It does not show the break in the curve that would indicate the beginning of turbulent flow. There is, however, other evidence which indicates the value of $N_{Re'}$ where turbulence begins. This evidence will be cited later.

Figure 5, which shows the effect of plotting the experimental calibration data on a modified Castleman plot when the temperature correlation factor is not used, illustrates the necessity of using a temperature-corrected resistance function to determine accurately the limits of laminar flow.

The experimental viscosities for methane and propane are given in Table 2 and are shown graphically in Figures 6 and 7; they were computed by use of Equation (12). The values of the viscometer calibration constant were determined by the statistical method of least squares, when one assumed that β was a straight-line function of temperature. Densities of liqiud methane and propane were obtained from the literature (*5*, *8*).

When turbulence begins in the viscometer, the fall times become greater than would be predicted, thereby giving values for viscosity which are too large. The deviation of the data on methane obtained with MM300 (Figure 6), starting at −140°C. and increasing with temperature, illustrates this. This deviation began at a modified Reynolds number of 285. On this basis the data obtained with MM308 should be reliable, since the highest experimental $N_{Re'}$ attained with this body was 209. Also the viscosity of propane at 80° and 90°C. measured with body MG303B would not be expected to be so reliable as the data obtained at lower $N_{Re'}$ because of the $N_{Re'}$ of 278 and 385 at these two temperatures. However, as can be seen in Figure 7, these two data points are not greatly in error with the data points taken at lower $N_{Re'}$.

The experimental error in determining the viscosity data presented is ±5% maximum for propane and ±8% maximum for methane. These figures are based upon the deviation of calibration data from the most probable values and the deviation of individual fall times from the mean.

CONCLUSIONS

The viscosity data for methane and propane have been obtained over temperature ranges where data were not previously available. Over temperature ranges where data were available the results obtained on the apparatus agree well with those in the literature.

By extensive and repeated calibrations of the viscometer the level of confidence in predicting the most probable value of the viscometer constant will be greatly improved. Since the greatest experimental error lies in the determination of the viscometer constant, the foregoing procedure would greatly reduce the present experimental error (±8% for methane and ±5% for propane).

ACKNOWLEDGMENT

The authors wish to express their gratitude to the Phillips Petroleum Company for its major contribution to this study, through both financial support and the gift of samples of materials.

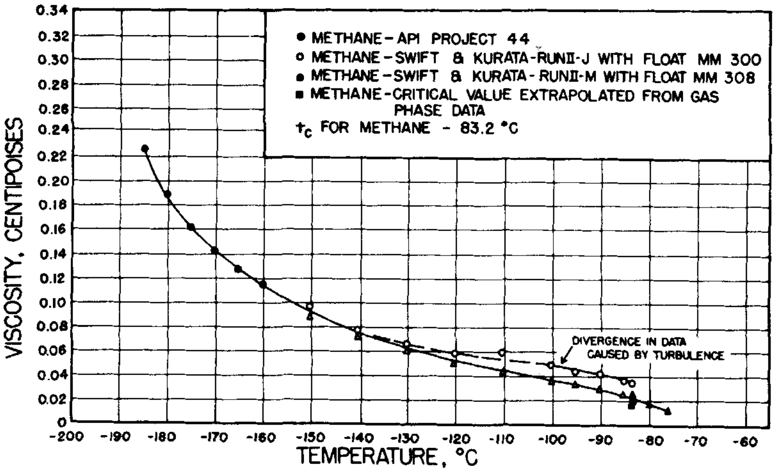

Fig. 6. Viscosity of liquid methane vs. temperature.

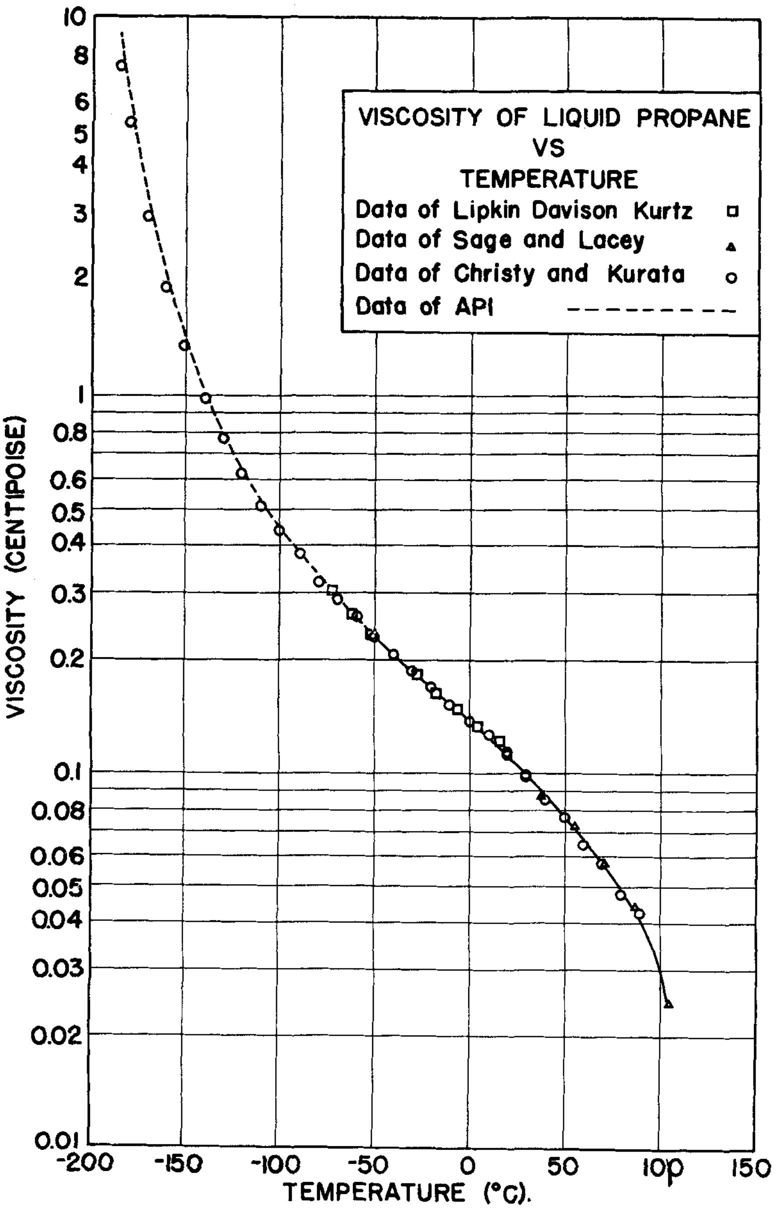

Fig. 7. Viscosity of liquid propane vs. temperature.

NOTATION

D = diameter of fall tube, cm.
d = diameter of falling body, cm.
f = resistance factor, dimensionless
f' = temperature corrected resistance factor, dimensionless
g = acceleration of gravity, cm./sec.^{2}
h = length of cylindrical portion of falling body, cm.
K = temperature correlation factor, dimensionless
N_{Re} = Reynolds number $dv\rho/\mu$, dimensionless
$N_{Re'}$ = modified Reynolds number $d^2s\rho/(D + d)\theta\mu$, dimensionless
s = timed interval of distance in viscometer cell, cm.
t = temperature, °C.
V = volume, cc.
v = average velocity of fluid, cm./sec.
W = resistance to motion, dynes

Greek Letters

β = viscometer calibration constant, sq. cm./sec.^{2}
β_0 = viscometer calibration constant at 0°C., sq. cm./sec.^{2}
δ = shape factor, dimensionless
θ = time, sec.
μ = viscosity, poise
ρ = density of fluid, g./cc.
σ = density of falling body, g./cc.
ψ = function, dimensionless
ϕ = function, dimensionless

LITERATURE CITED

1. Barr, Guy, "A Monograph of Viscometry," Humphrey Milford, London (1931).
2. Bridgeman, P. W., "The Physics of High Pressure," G. Bell and Sons, Ltd., London (1931).
3. "Handbook of Chemistry and Physics," 30 ed., pp. 1697, 1736, Chemical Rubber Publishing Co., Cleveland, Ohio (1948).
4. Hubbard, R. M., and G. G. Brown, *Ind. Eng. Chem. Anal. Ed.*, **15**, 212 (1943).
5. Matthews, C. S., and C. O. Hurd, *Trans. Am. Inst. Chem. Engrs.*, **42**, 55 (1946).
6. Natural Gasoline Assn. of America, Tech. Committee, *Ind. Eng. Chem.*, **34**, 1240 (1942).
7. Rayleigh, J. W. S., *Phil. Mag.*, **36**, 365 (1893).
8. Rossini, F. D., *Am. Petroleum Inst. Research Project* 44, Carnegie Press, Pittsburgh, Pennsylvania (1953).
9. Sage, B. F., and W. N. Lacey, *Ind. Eng. Chem.*, **30**, 829 (1938).
10. Stokes, G. G., "Mathematical and Physical Papers," Vol. 3, University Press, Cambridge (1901).
11. Swift, G. W., *et al.*, *Chem. Eng. Progr.*, **54**, 6, 47 (June, 1958).

Manuscript received September 25, 1957; revision received March 3, 1958; paper accepted March 13, 1958. Paper presented at A.I.Ch.E., Baltimore meeting.